Astroglia in Medullary Dorsal Horn (Trigeminal Spinal Subnucleus Caudalis) Are Involved in Trigeminal Neuropathic Pain Mechanisms

Akiko Okada-Ogawa[1,2], **Ikuko Suzuki**[3], **Barry J. Sessle**[5,6], **Chen-Yu Chiang**[5], **Michael W. Salter**[5,6,7], **Jonathan O. Dostrovsky**[5,6], **Yoshiyuki Tsuboi**[3,4], **Masahiro Kondo**[3,4], **Junichi Kitagawa**[3,4], **Azusa Kobayashi**[1,2], **Noboru Noma**[1,2], **Yoshiki Imamura**[1,2], and **Koichi Iwata**[3,4,8]

[1]Department of Oral Diagnosis, Nihon University School of Dentistry, Chiyoda-ku, Tokyo 101-8310, Japan

[2]Division of Oral Health Science, Dental Research Center, Nihon University School of Dentistry, Chiyoda-ku, Tokyo 101-8310, Japan

[3]Department of Physiology, Nihon University School of Dentistry, Chiyoda-ku, Tokyo 101-8310, Japan

[4]Division of Functional Morphology, Dental Research Center, Nihon University School of Dentistry, Chiyoda-ku, Tokyo 101-8310, Japan

[5]Faculty of Dentistry, University of Toronto, Toronto, Ontario M5G 1G6, Canada

[6]Department of Physiology, University of Toronto, Toronto, Ontario M5S 1A8, Canada

[7]Program in Neuroscience and Mental Health, Hospital for Sick Children, Toronto, Ontario M5G 1X8, Canada

[8]Division of Applied System Neuroscience, Advanced Medical Research Center, Nihon University Graduate School of Medical Science, Itabashi-ku, Tokyo 173-8610, Japan

Abstract

The aim of this study was to investigate whether astroglia in the medullary dorsal horn (trigeminal spinal subnucleus caudalis; Vc) may be involved in orofacial neuropathic pain following trigeminal nerve injury. The effects of intrathecal administration of the astroglial aconitase inhibitor sodium fluoroacetate (FA) were tested on Vc astroglial hyperactivity [as revealed by glial fibrillary acid protein (GFAP) labeling], nocifensive behavior, Vc extracellular signal-regulated kinase phosphorylation (pERK), and Vc neuronal activity in inferior alveolar nerve-transected (IANX) rats. Compared with sham-control rats, a significant increase occurred in GFAP-positive cells in ipsilateral Vc at postoperative day 7 in IANX rats, which was prevented following FA administration. FA significantly increased the reduced head withdrawal latency to high-intensity heat stimulation of the maxillary whisker pad skin in IANX rats, although it did not significantly affect the reduced escape threshold to low-intensity mechanical stimulation of the whisker skin in IANX rats. FA also significantly reduced the increased number of pERK-like immunoreactive cells in Vc and the enhanced Vc nociceptive neuronal responses following high-intensity skin stimulation that were documented in IANX rats, and glutamine administration restored the enhanced responses. These

Correspondence should be addressed to Dr. Koichi Iwata, Department of Physiology, Nihon University School of Dentistry, 1-8-13 Kanda-Surugadai, Chiyoda-ku, Tokyo 101-8310, Japan. iwata-k@dent.nihon-u.ac.jp .

various findings provide the first documentation that astroglia is involved in the enhanced nociceptive responses of functionally identified Vc nociceptive neurons and in the associated orofacial hyperalgesia following trigeminal nerve injury.

Introduction

There are many reports that hyperactivity of non-neuronal (glial) cells is involved in the neuroplastic changes reflecting hyperexcitability of Vc nociceptive neurons in the medullary dorsal horn (trigeminal spinal subnucleus caudalis; Vc) and spinal dorsal horn (DH) following peripheral nerve injury. While glial cells are known to have important functions in nourishing and supporting neurons (Allen and Barres, 2005; Fitzgerald, 2005; Araque, 2006; Haydon and Carmignoto, 2006), many recent studies have reported that hyperactive glial cells are involved in modulating Vc and spinal DH neuronal activity after peripheral nerve injury or inflammation (Watkins and Maier, 2003; Ji, 2004; Ji and Strichartz, 2004; Tsuda et al., 2005; Piao et al., 2006; Chiang et al., 2007, 2008; Xie et al., 2007; Wei et al., 2008).

Following peripheral nerve injury, glial cells in the Vc and spinal DH are hyperactive and may change their morphological features and manifest large somata with many thick processes (Jongen et al., 2007; Xu et al., 2008). Various chemical mediators are released from hyperactive glial cells following a variety of stimuli and some [e.g., brain-derived factor (BDNF) and glutamine] are involved in the modulation of Vc and spinal DH neuronal excitability (Sharma, 2005; Chiang et al., 2007). It is known that the tricarboxylic acid (TCA) cycle in astroglia converts glucose to glutamate through the action of the enzyme aconitase, and the subsequent production and release of glutamine is then trafficked through transporters into glutamatergic nerve terminals where glutamine is hydrolyzed to form glutamate to replenish the glutamate transmitter pool (Fonnum et al., 1997; Schousboe and Waagepetersen, 2006). Inhibitors of aconitase such as fluoroacetate (FA) reduce the production of glutamine from glucose and have been reported to prevent formalin-induced hyperalgesia and nerve inflammation-induced pain (Watkins and Maier, 2003; Ji, 2004; Tsuda et al., 2005). These findings suggest that aconitase and the astroglia-dependent glutamine supply to neurons could be relevant in sustaining enhanced neuronal activity related to chronic pain mechanisms.

It has been also documented that the application to Vc of fluoroacetate or another potent astroglial inhibitors methionine sulfoximine (MSO) significantly reduces the enhanced Vc neuronal excitability reflecting central sensitization in rats with tooth pulp inflammation (Chiang et al., 2007; Xie et al., 2007). Since astroglia in Vc may also be hyperactive following trigeminal nerve injury as well as orofacial inflammation (Piao et al., 2006; Guo et al., 2007; Wei et al., 2008), the aim of the present study was to examine the effect of the astroglial inhibitor fluoroacetate on mechanical- and heat-induced nocifensive behavior, Vc hyperactive astroglial cells and Vc nociceptive neuronal activity in inferior alveolar nerve-transected (IANX) rats. In addition, we also analyzed phosphorylation of extracellular signal-regulated kinase (ERK), which is one of the mitogen-activated protein kinases (MAPKs) activated by calcium influx (Rosen et al., 1994; Ji et al., 1999). ERK phosphorylation is known to be induced in spinal DH and Vc neurons by noxious stimulation (Ji et al., 1999; Shimizu et al., 2006; Noma et al., 2008).

Materials and Methods

This study was approved by the Animal Experimentation Committee at Nihon University School of Dentistry, and procedures were performed according to the guidelines of the International Association for the Study of Pain (Zimmermann, 1983).

Adult male Sprague Dawley rats weighing 280–380 g were used in the neuron recording, immunohistochemical and behavioral experiments (supplemental Fig. S1, available at www.jneurosci.org as supplemental material) and animal preparation were performed by different experimenters, and the subsequent experimental procedures were conducted under blind conditions.

Sodium FA (Sigma-Aldrich) as the astroglial aconitase inhibitor was dissolved with isotonic saline (1 m$_M$) and used for continuous or single intrathecal injection. The same isotonic saline solution also was used as the vehicle control for FA.

Inferior alveolar nerve transection

Our previous procedures (Iwata et al., 2001) were used for the IAN transection. Briefly, rats were initially anesthetized with sodium pentobarbital (50 mg/kg, i.p.) and then were placed on a warm mat, a small incision was made on the surface of the facial skin and the masseter muscle, and the surface of the alveolar bone covering the IAN was removed to expose the IAN. The IAN was tightly ligated at two points of the nerve trunk at just above the angle of the mandible and 1 mm proximal from the angle of the mandibular bone, and then transected. Sham-control rats were also used: the facial skin and the masseter muscle were similarly incised and the surface of the alveolar bone was removed, but no IAN transection was carried out. After surgery, penicillin G potassium (20,000 U, i.m.) was injected to prevent infection.

Behavioral testing

As we have previously described (Iwata et al., 2001; Tsuboi et al., 2004), IANX rats show reduced escape threshold to mechanical stimulation of the maxillary whisker pad skin. Therefore, we measured the escape threshold to mechanical stimulation of the maxillary whisker pad skin and head withdrawal latency to heat stimulation or head withdrawal latency to high-intensity heat stimulation of the maxillary whisker pad skin in lightly anesthetized rats that received intrathecal administration of FA or vehicle (isotonic saline) to evaluate mechanical allodynia (continuous i.t. injection of FA or saline; single i.t. injection of FA or saline, $n = 5$ in each group) in IANX rats and heat hyperalgesia in IANX rats (continuous i.t. injection of FA or saline for 7 d in awake IAN rats; single i.t. injection of FA or saline in lightly anesthetized IANX rats, $n = 5$ in each group) and lightly anesthetized sham-control rats (single i.t. administration of FA or isotonic saline, $n = 5$ each).

The test for nocifensive behavior following IAN transection has been previously described (Iwata et al., 2001). Rats were trained daily to stay in a plastic cage for 20 min and protrude their perioral regions including the maxillary whisker pad through a hole made in the wall of the plastic cage for 5–10 min. For training related to the mechanical escape threshold measurement, a series of von Frey filaments was used for mechanical stimulation of the maxillary whisker pad skin, which we previously documented as associated with a reduced escape threshold in IANX rats (Iwata et al., 2001; Nomura et al., 2002). After 1 week of training, rats became capable of receiving the mechanical stimuli during protrusion of their perioral regions. The criterion performance was when the rats could keep their nose protruding for 5–10 min without escape from high-intensity mechanical stimulation applied by the von Frey hair to the maxillary whisker pad skin. Since each rat had a different escape threshold to mechanical stimulation, the maximum stimulus intensity differed between rats (15–75.8 g). All rats showed escape behavior when a 75.8 g stimulus was applied to the maxillary whisker pad skin, and so 75.8 g was the strongest stimulus intensity used for the nocifensive behavioral test. The daily training sessions took place until criterion performance was reached. At this time, IAN transection was performed as well as insertion of the mini-osmotic pumps to test the effect of FA on mechanical escape threshold. The soft microsilicon tube (0.8 mm in diameter) for FA administration was inserted under the pia mater at the same time as IAN

transection. Under pentobarbital anesthesia (50 mg/kg, i.p.), a laminectomy was performed at the L5 spinal cord and the dura was opened. A microsilicon tube was inserted beneath the pia mater until the tip of the microsilicon tube could be seen to reach the C1 spinal cord. A microsilicon tube was connected to the mini-osmotic pump (Alzet model 2001, Durect; total volume of the pump: 200 µl, drug infusion: 1 µl/h for 7 d), which was filled with 1 m$_M$ FA or isotonic saline and embedded subcutaneously in the dorsal portion of the rat's body; FA or isotonic saline was continually applied intrathecally to the subdural space for 7 d. The behavioral experiment was conducted in rats without any motor deficit. The threshold for escape behavior to mechanical stimulation of the maxillary whisker pad skin was measured before IAN transection and then at 1–7 d, as well as 10, 14, 21, and 28 d after IAN transection. The mechanical escape threshold in each test period was described as a percentage of that before IAN transection. The Alzet pump was removed after the behavioral testing, and the amount of FA remaining in the pump was measured to verify that a daily dose of 24 µl(1 µl/h) FA had been delivered. If FA remained in the pump, the data from that rat were excluded from the analysis. We also tested the effects of continuous intrathecal administration of 1 m$_M$ FA or vehicle (isotonic saline) on the head withdrawal latency to heat stimulation of the maxillary whisker pad skin in IANX rats at 7 d after IAN transection ($n = 5$ in each group), and the mean difference score of head withdrawal latency (contralateral — ipsilateral) was calculated.

Our previous procedures (Ogawa and Meng, 2009) were used to study heat hyperalgesia and the effect of FA. Briefly, a soft microsilicon tube was inserted intrathecally from the L5 into the C1 level at 4 d before behavioral testing in IANX or sham-control rats; the IAN transection or sham operation had been performed 3 d before microsilicon tube insertion. Rats were lightly anesthetized with urethane (1.16 g/kg, i.p.) at 7 d after the IAN transection (or sham operation) and bipolar enamel-coated silver wire-electrodes (interelectrode distance: 5–6 mm) were placed in the splenius capitis muscle for electromyographic (EMG) recording. As previously described (Saito et al., 2008), a heat stimulus (50°C) was applied to the maxillary whisker pad skin through a contact heat probe (5 mm in diameter). After stable baseline controls, intrathecal administration of 1 m$_M$ FA or (isotonic saline) was delivered in a total volume of 10 µl followed by a 10 µl saline flush. The head withdrawal latency was measured from the onset of the heat stimulus to the onset of neck EMG activity in IANX and sham-control rats before and 30 and 60 min after drug administration (cutoff latency = 30 s). The maximal possible analgesic effect (MPE) was calculated from the following formula: MPE (%) = (test latency — control latency)/(cutoff — control latency) $\times$ 100. We also tested the effects of continuous intrathecal administration of 1 m$_M$ FA or vehicle (isotonic saline) on the head with-drawal latency to heat stimulation of the maxillary whisker pad skin in IANX rats at 7 d after IAN transection ($n = 5$ in each group).

GFAP, pERK, and NeuN immunohistochemistries

GFAP is a specific marker of astroglial cells (Piao et al., 2006; Guo et al., 2007). At 1 or 7 d after IAN transection or 7 d after sham operation, the rats received intrathecal administration of 1 m$_M$ FA ($n = 5$) or vehicle (isotonic saline) ($n = 5$) delivered in a total volume of 10 µl followed by a 10 µl saline flush and then were anesthetized with sodium pentobarbital (50 mg/kg, i.p.) and perfused through the aorta with isotonic saline (500 ml) followed by 4% paraformaldehyde in 0.1 $_M$ phosphate buffer (PB, pH 7.4, 500 ml). The medulla and upper cervical cord were removed and postfixed in 4% paraformaldehyde for 3 d at 4°C. The tissues were then transferred to 20% sucrose (w/v) in PBS for several days for cryoprotection. Thirty-micrometer-thick sections of the caudal medulla and upper cervical spinal cord from IANX rats (1 and 7 d after IAN transection), sham-control rats (7 d after sham operation), or 7 d IANX rats with FA or vehicle (isotonic saline) administration (administrated as described above) ($n = 5$ each) were processed with GFAP immunohistochemistry. Sections were incubated in rabbit

anti-GFAP (1:1000; Dako Z0334) for 2 d at 4°C with agitation. Then sections were incubated in anti-rabbit Alexa Fluor 568 IgG (1:200; Invitrogen) and after washing were mounted and cover-slipped. The density of the GFAP-labeled astroglial cells in Vc was measured by using a computer-assisted imaging analysis system (NIH Image, version 1.61). Measurements were made in a $100 \times 100\,\mu m^2$ region of Vc that receives afferents from the second and third branches of the trigeminal nerve and that contains the densest labeling of astroglia (see Noma et al., 2008) as illustrated in Figure 1.

For pERK immunohistochemistry in IANX rats at 7 d after IAN transection or in sham-control rats, with intrathecal infusion of FA or isotonic saline, rats received low-intensity (von Frey hair 6 g) or high-intensity (von Frey hair 75.8 g) mechanical stimulation of the maxillary whisker pad skin (1 Hz, duration for 10 min) to evoke activity in that part of Vc receiving afferent input from the second branch of the trigeminal nerve. Then, 5 min later they were perfused and 30-µm-thick sections were cut with a freezing microtome and every fourth section was collected in PBS. Free-floating tissue sections were rinsed in PBS, incubated in 10% normal goat serum in PBS for 1 h, and then incubated in rabbit anti-phospho-p44/42 MAP kinase (Thr202/Tyr204) antibody (1:1000) for 72 h at 4°C. Next, the sections were incubated in biotinylated goat anti-rabbit IgG (1:600; Vector Laboratories) for 2 h at room temperature. After washing, the sections were incubated in peroxidase-conjugated avidin–biotin complex (1:100; ABC, Vector Laboratories) for 1 h at room temperature. They were then washed in 0.05 M Tris buffer (TB), and next incubated in 0.035% 3,3'-diaminobenzidine-tetra HCl (DAB, Tokyo Chemical Industry), 0.2% nickel ammonium sulfate, and 0.05% peroxide in 0.05 M TB, pH 7.4. The sections were then washed in PBS, serially mounted on gelatin-coated slides, dehydrated in a series of alcohols (from 50 to 100%), and coverslipped. The pERK-like immunoreactive (pERK-LI) cells were drawn under a light microscope (objective: 10× or 20×) with an attached camera lucida drawing tube (Neurolucida 2000 MicroBrightField). The number of all pERK-LI cells in Vc and upper cervical spinal cord was counted from three of every six sections, and the mean number of pERK-LI cells (per three sections per rat) was calculated from each animal, to reduce the variability of the number of immunoreactive neurons in each section.

Double-immunofluorescence histochemistry was also used to determine whether the pERK-LI cells expressed a neuronal label. IANX rats with intrathecal infusion of FA ($n = 5$) or isotonic saline ($n = 5$) received high-intensity mechanical stimulation of the maxillary whisker pad skin (1 Hz, duration for 10 min) and 5 min later were perfused and 30-µm-thick sections of the caudal medulla and upper cervical spinal cord were cut with a freezing microtome and processed for double-labeling immunohistochemistry for pERK and the neuronal label NeuN in that region of Vc receiving afferent input from the second branch of the trigeminal nerve. Free-floating tissue sections were rinsed in PBS, incubated in 10% normal goat serum in PBS for 1 h, and then incubated in rabbit anti-phospho-p44/42 MAPK antibody (1:300; Cell Signaling Technology) and mouse anti-NeuN antibody (1:1000; Millipore Bioscience Research Reagents), or mouse anti-phospho-p44/42 MAP kinase antibody (1:500, Cell Signaling Technology) and rabbit anti-Iba1 antibody (1:2000, Wako) or rabbit anti-GFAP polyclonal antibody (1:5000, Dako) overnight at 4°C and secondary antibodies (anti-rabbit Alexa Fluor 488 IgG and anti-mouse Alexa Fluor 568, 1:200; Invitrogen) conjugated for 1 h at room temperature in a dark room. Then the sections were washed in PBS three times for 5 min. Sections were mounted on slides and coverslipped in PermaFluor (Sigma). The number of NeuN-LI and pERK-LI double-labeled cells was counted in the rats receiving noxious mechanical stimulation (75.8 g) of the face.

Vc neuronal recording

Previously described procedures (Iwata et al., 2001) were used in IANX rats ($n = 17$) and sham-control rats ($n = 11$) for an acute single-neuron recording experiment. Briefly, rats were initially anesthetized with sodium pentobarbital (50 mg/kg, i.p.), and the trachea and right femoral vein were cannulated to allow artificial respiration and intravenous administration of drugs. Anesthesia was maintained with isoflurane (2–3%) mixed with oxygen during surgery. Rats were mounted in a stereotaxic frame, the medulla was exposed by a laminectomy, and dura and pia mater were removed from the exposed brain surface.

Rats were anesthetized with continuous inhalation of 2–3% isoflurane mixed with oxygen. Animals were immobilized with pancuronium bromide (0.6 mg/kg, i.v.) and artificially ventilated. End-tidal CO_2 was maintained from 3.5 to 4.5%. The rectal temperature was maintained at 37°C by a feedback-controlled heating blanket. The electrocardiogram was monitored and the heart rate was maintained at 250–300/min. If the heart rate was increased during mechanical or thermal stimulation, the concentration of isoflurane was increased appropriately. A laminectomy was performed to expose Vc, and a pool was made with skin flaps around the laminectomy, and the brainstem kept moist with vehicle solution (isotonic saline). A PE-50 catheter was placed at the level of obex to infuse or suck out drugs during recording. Single neuronal activity was recorded using tungsten microelectrodes (impedance $= 13$ MΩ, 1000 Hz) from histologically determined sites in Vc, as previously described (Iwata et al., 2001). Neurons were functionally identified as wide dynamic range (WDR) neurons or nociceptive-specific (NS) neurons by their responses to innocuous or noxious mechanical stimulation of their receptive fields (RFs), as previously described (Trevino et al., 1973; Iwata et al., 2001; Chiang et al., 2007). The WDR neurons responded to innocuous stimuli and to a greater degree to noxious stimuli. The NS neurons responded only to noxious stimuli. The single neuronal activity was amplified using a differential amplifier (Nihon Koden) and stored in the microcomputer hard disk. Spikes were sorted and spike frequencies were analyzed using the Spike II software (CED 1401, UK).

We only focused on Vc neurons with RFs in the maxillary whisker pad skin. After identification of WDR or NS neurons, mechanical and thermal stimuli were applied to the lowest threshold area of the neuronal RF. For mechanical stimulation, low-intensity graded stimuli with von Frey filaments (1.2, 5.4, and 15.1 g) and brushing with a camel-hair brush were applied for 5 s at 10 s intervals. High-intensity stimulation with von Frey filaments (28.8 and 75.8 g) and pinch produced by a small arterial clip were also applied for 5 s at 10 s intervals. For thermal stimulation, weak heating (44°C and 46°C) and cooling (20°C and 30°C) stimuli were applied for 10 s by a contact thermode (Iwata et al., 1999). Strong noxious heating (48°C and 50°C) and 10°C cold stimulation were applied for 10 s, and 3 min were interposed between the thermal stimuli to avoid sensitization of peripheral nociceptors.

After the properties of Vc single neurons were defined in each experiment, the pool covering the Vc region was filled with vehicle (isotonic saline) and then 1 m$_M$ FA (0.6 ml/h) was continually perfused over the Vc surface for 30–60 min after the vehicle (isotonic saline), as described by Chiang et al. (2007). Any changes in spontaneous activity, mechanicalevoked responses, and cold- or heat-evoked responses were analyzed before, during, and after the vehicle (isotonic saline) or FA infusion. FA or vehicle (isotonic saline) infusion was discontinued after the neuronal testing. To test whether glutamine could reverse any FA-induced effects, 15 min after FA infusion, glutamine (4 mg/ml) was continually infused for 15 min ($n = 5$). Then the pinch-evoked responses were analyzed. To evaluate the recovery of neuronal activity after washout of FA in IANX rats, WDR neuronal activities were recorded for a further 60 min after washout of FA and checked any subsequent change in spike frequencies.

Statistical analysis

Spike frequencies were analyzed only in WDR neurons but not NS and LTM neurons because of insufficient number of NS and LTM neurons for statistic analysis. Results are presented as means ± SEM. Statistical analysis was performed by two-way ANOVA using time as a repeated measurement, and followed by Dunnett's test for the behavioral data of mechanical stimulation, evoked Vc neuronal responses, and behavioral data of thermal stimulation. Student's *t* test or Welch's *t* test was conducted when two groups were compared (analysis for GFAP immunohistochemistry, the number of pERK-LI cells, background activities, and Vc neuronal RF sizes). Differences were considered significant at $p < 0.05$.

Results

Hyperactive astroglia in Vc

Astroglia as reflected by cells showing GFAP labeling had a large soma with thick processes, and the area occupied by the GFAP-labeled cells in IANX rats 7 d after the IAN transection (Fig. 1 *G–I*) was much larger than that observed in sham-control rats 7 d after the sham operation (Fig. 1 *A–C*) and IANX rats 1 d after IAN transection (Fig. 1 *D–F*)(*n* = 5 in each group). The Vc was subdivided in relation to three parts expressing pERK-LI cells following capsaicin injections to first, second, and third branches of the trigeminal nerve-innervated facial skin, according to the criteria by Noma et al. (2008). GFAP-labeled cells at 7 d after IAN transection were widely distributed within that part of Vc receiving afferent inputs from both second and third branches of the trigeminal nerve, and the area occupied by the GFAP-labeled cells in this part of Vc was significantly larger in the Vc of IANX rats at 7 d after transection compared with that of 1 d IANX rats and of sham-control rats 7 d after sham operation (Fig. 1 *J*).

In contrast to the large area occupied by GFAP-labeled immunoproducts observed in Vc of IANX rats at 7 d after IAN transection following intrathecal administration of vehicle (isotonic saline) (Fig. 2 *A,B*), the area occupied by GFAP-labeled immunoproducts in Vc was significantly decreased following intrathecal administration of FA for 7 d (24 µl/d) in the IANX rats at 7 d after IAN transection (Fig. 2 *C–E*) (*n* = 5).

Nocifensive behavior

The escape threshold to low-intensity mechanical stimulation of the maxillary whisker pad skin was significantly reduced after IAN transection compared with that before IAN transection in intrathecal FA- and intrathecal vehicle (isotonic saline)-administered IANX rats, and the lowering of escape threshold in IANX rats lasted at least for 28 d after the IAN transection (Fig. 3*A*)(*n* = 5 in each group). The mechanical escape threshold in IANX rats was reversed at 6–21 d after IAN transection following continuous intrathecal infusion of FA, but not significantly compared with the effects of vehicle (isotonic saline) control (Fig. 3*A*). We also tested the single FA intrathecal administration on mechanical nocifensive behavior before and 7 d after IAN transection in IANX rats (IANX, saline, *n* = 5 in each group). We could not observe any changes in mechanical escape threshold after single intrathecal FA administration compared with that before FA injection (Fig. 3*B*). On the other hand, the mean difference score of heat-induced head withdrawal latency was significantly smaller in the rats with continuous FA intrathecal infusion at 7 d after IAN transection compared with vehicle-infused rats (Fig. 3*C*)(*n* = 5 in each group). The MPE to noxious heating of the maxillary whisker pad skin was also significantly increased at 30 and 60 min after intrathecal administration of FA but not in sham-control rats compared with that of intrathecal vehicle (isotonic saline), indicating that nocifensive behavior was depressed in FA-administrated rats (Fig. 3*D,E*)(*n* = 5 in each group).

were not changed in sham-control rats following intrathecal vehicle (isotonic saline) or FA administration (Fig. 6*A*). On the other hand, heat-evoked responses were depressed in IANX rats following bath application of FA, but not following bath application of vehicle (isotonic saline) (Fig. 6*B*). Heat-evoked responses at 44 and 46°C were not significantly different between IANX and sham-control rats during vehicle (isotonic saline) administration (Fig. 6 *C,D*, Vehicle), whereas those at 48 and 50°C were significantly larger in IANX rats compared with those of sham-control rats, again consistent with the presence of hyperexcitability of Vc nociceptive neurons in the IANX rats (Fig. 6*E,F*, Vehicle). The mean peak discharges evoked by 44 and 46°C stimulation of the maxillary whisker pad skin were not affected by bath application of FA in IANX rats (Fig. 6*C,D*), whereas those of 48 and 50°C stimulation were significantly depressed 30–60 min after bath application of FA in IANX rats (Fig. 6 *E, F*). We could not observe any changes in heat-evoked responses after bath application of vehicle in sham-control and in IANX rats (Fig. 6 *C–F*).

Cold-responses were also depressed by bath application of FA in IANX rats, as illustrated in Figure 7. We could not observe any changes in cold-evoked (10°C) responses after bath application of vehicle or FA in sham-control rats (Fig. 7*A*), whereas a strong depression of cold-evoked (10°C) responses was observed 30–60 min after bath application of FA in IANX rats (Fig. 7*B*). The vehicle administration did not cause any changes in cold-evoked (10°C) responses in IANX rats (Fig. 7*B*). The cold-evoked responses were not different between IANX rats and sham-control rats during vehicle administration (Fig. 7*C–E*). The peak discharges evoked by 20°C stimulation were significantly depressed at 30 min after bath application of FA in IANX rats compared with sham-control rats (Fig. 7*D*). We could not observe differences in 30°C responses after FA administration in IANX and sham-control rats (Fig. 7*E*). The background activity and the RF size were not affected by administration of FA (data not shown).

We also tested the effect of the medullary infusion of glutamine on pinch-evoked responses, as illustrated in Figure 8. Pinch-evoked responses were not affected by administration of vehicle in the IANX rats but were depressed 60 min after administration of FA (Fig. 8 *A*). The depression of pinch-evoked responses by FA was not reversed when vehicle was administered after FA, whereas a larger pinch-evoked response was observed after glutamine infusion (Fig. 8 *A*). The mean peak firing frequencies before and after FA glutamine are illustrated in Figure 8 *B*. The pinch-evoked responses were significantly decreased after intrathecal administration of FA in IANX rats compared with vehicle (isotonic saline) infusion, but this effect was significantly reversed after superfusion of glutamine administration.

Discussion

This study has provided novel evidence suggesting a role for astroglia and the glutamate–glutamine shuttle in mediating the hyperexcitability of Vc nociceptive neurons resulting from IAN injury. Several different experimental strategies were used to investigate the possible role of astroglia in mediating the hyperexcitability of Vc nociceptive neurons induced by IAN transection. Inhibition of astroglial function by administration of FA was able to reverse IAN transection-induced changes in hyperactive astroglia, nocifensive behavior, pERK expression, and responses to noxious stimuli reflecting hyperexcitability of Vc nociceptive neurons of functionally identified single Vc nociceptive neurons. Furthermore, administration of glutamine was found to block the FA effects on IANX-induced neuronal hyperexcitability.

Technical considerations

The volume of FA continually infused was small (1 µl/h) and the tip of the microsilicon tube was positioned in the caudal medulla near the Vc. The small FA volume and localized application site favor the view that the action of FA was on sites in Vc or immediately adjacent

regions, although we cannot rule out the possibility that the FA may have diffused to involve also more distant sites in the caudal brainstem or upper cervical spinal cord. It is unlikely that the observed Vc neuronal and behavioral effects of FA could be attributed to neurotoxic effects of FA since FA caused no change in baseline properties of Vc neurons, consistent with our earlier data, or in neuronal and behavioral responses to low-intensity mechanical stimuli, which might be expected if FA at the dosage used was having toxic effects on neurons. The rapid recovery of neuronal properties typical of IANX rats, following washout of FA, is also consistent with this view.

We analyzed the GFAP immunoproducts in Vc to detect the hyperactive astroglia. However, GFAP has been reported to be expressed in the Schwann cells as well as astroglial cells (Cheng and Zochodne, 2002). Therefore, we cannot exclude the possibility that the GFAP immunoproducts in the Vc include Schwann cells as well as astroglial cells.

Time course change in hyperactive astroglial cells

Previous studies have shown that peripheral nerve injury causes strong hyperactivity of microglia and astroglia in the Vc and spinal DH (Piao et al., 2006; Ji et al., 2007; Xu et al., 2008). These glial cells are known to be hyperactive with different time courses after the nerve injury (Piao et al., 2006; Wei et al., 2008). The morphological features of glial cells change in the hyperactive state, with a large cell body and thick processes during the hyperactive stage. Many previous papers have reported that the hyperactive glial cells have functional interactions with neurons in many CNS regions (Newman, 2003; Perea and Araque, 2006; Wei et al., 2008). While as noted above, it has been also reported that microglia and astroglia are hyperactive in Vc after IAN transection (Piao et al., 2006), it is still unknown how glial cells and Vc nociceptive neurons communicate with each other following trigeminal nerve injury. In the present study, we focused on hyperactive astroglial cells in the Vc following IAN transection. We observed a significant increase in the area occupied by GFAP-positive cells in Vc at 7 d after the IAN transection but not at 1 d after IAN transection. Since GFAP is a reliable marker for astroglial cells (Debus et al., 1983; Franke et al., 1991; Piao et al., 2006), this finding suggests that astroglia in Vc are hyperactive 7 d after trigeminal nerve injury. Together with previous data (Chiang et al., 2007; Xie et al., 2007), the present results suggest that the astroglia may be involved in an enhancement of Vc neuronal activity at the very early period within 2 h and also in the later period after trigeminal nerve injury. It has been reported that glial cell hyperactivity is produced faster in microglia than astroglia and that astroglial hyperactivity is longer lasting, suggesting that hyperactive astroglial cells in Vc produced by the IAN transection may be involved in maintenance of the trigeminal neuropathic pain state rather than initiation of neuropathic pain. However, our previous studies have implicated astroglial cells also in initiating acute hyperexcitability of Vc nociceptive neurons occurring within 10 min of application of the inflammatory irritant mustard oil to the tooth pulp (Chiang et al., 2007; Xie et al., 2007). These previous single-neuron recording studies also revealed that intrathecal administration of potent astroglial cell inhibitors MSO or FA causes significant reduction in tooth pulp stimulation-induced hyperexcitability of Vc nociceptive neurons in rats (Chiang et al., 2007; Xie et al., 2007).

Modulation of Vc neuronal activity

We used the astroglial inhibitor FA to clarify the involvement of astroglial hyperactivity in Vc neuronal activity and nocifensive behavior in rats with IAN transection. We observed a significant reduction in the Vc area occupied by GFAP-positive cells after FA infusion. The significant decrease in nocifensive behavior to noxious heat stimulation of the maxillary whisker pad skin was also obvious in IANX rats. We also have preliminary data that intrathecal MSO administration causes significant reduction of high-intensity mechanical-evoked Vc neuronal responses (data not shown), consistent with recent findings that intrathecal MSO can

suppress nociceptive Vc neuronal activity (Chiang et al., 2007). These findings suggest that the hyperactive astroglia are mainly involved in modulation of nociceptive responses of nociceptive neurons in Vc after trigeminal nerve injury.

We also studied the effect of FA administration on ERK phosphorylation in Vc neurons following high-intensity mechanical stimulation of the maxillary whisker pad skin. ERK is phosphorylated within 10 min by a variety of noxious stimuli in Vc as well as spinal DH neurons following noxious stimulation (Shimizu et al., 2006; Suzuki et al., 2007; Noma et al., 2008). We observed many pERK-LI cells in the Vc following high-intensity mechanical stimulation of the maxillary whisker pad skin, but there was a marked reduction in such cells following FA administration. On the other hand, no changes in pERK-LI cell expression after FA administration were seen in IANX rats after low-intensity mechanical stimulation and in sham-control rats after high-intensity stimulation.

Since it is well known that Vc nociceptive neurons can be sensitized by IAN transection, resulting in allodynia and hyperalgesia in the maxillary whisker pad skin (Iwata et al., 2001; Nomura et al., 2002; Tsuboi et al., 2004), the present results indicate that only nociceptive responses are strongly depressed by FA, suggesting that hyperactive astroglia are involved in the hyperalgesia induced by the hyperexcitability of Vc neurons following trigeminal nerve injury. This is consistent with our earlier findings of FA (or MSO) reversing hyperexcitability of Vc nociceptive neurons induced by acute tooth pulp stimulation (Chiang et al., 2007; Xie et al., 2007). It is also consistent with our behavioral data showing that only behavioral responses to high-intensity stimulation were influenced by the FA administration. Collectively, the neuronal and behavioral findings indicate that the astroglia may be differentially affecting high-threshold versus low-threshold afferent inputs to Vc nociceptive neurons and the associated behavioral responses in this IANX model. Further studies are needed to ascertain whether this differential effect can be explained by astroglial presynaptic versus postsynaptic actions on Vc neurons.

Involvement of glutamine–glutamate shuttle

We also observed that the glutamine superfusion significantly restored the increased excitability of Vc nociceptive neurons that has been reported in IANX rats by FA superfusion, and this is consistent with previous findings of glutamine effectiveness reversing MSO-induced inhibition in tooth pulp-stimulated rats (Chiang et al., 2007), and provides further evidence of the importance of the astroglial glutamine–glutamate shuttle in acute and chronic pain models (Hertz and Zielke, 2004; Fonseca et al., 2005).

Many previous papers have reported that astroglial cells convert glucose to glutamate through the action of aconitase in the TCA cycle, and then glutamate is converted to glutamine, which is released into the extracellular space and taken up by presynaptic glutamatergic terminals (Martinez-Hernandez et al., 1977; Keyser and Pellmar, 1994; Hertz and Zielke, 2004; Fonseca et al., 2005). FA is known to inhibit the action of aconitase in the astroglial TCA cycle, which leads to a reduction in the formation and release of glutamine by the astroglial cells and eventually a reduction of glutamate used by neurons (Swanson and Graham, 1994; Fonnum et al., 1997; Schousboe et al., 1997). Previous studies have reported that FA prevents formalin-induced hyperalgesia evoked by proinflammatory substances (Watkins et al., 1997; Milligan et al., 2003; Watkins and Maier, 2003) and suppresses synaptic excitability and spontaneous activity in hippocampal neurons (Bacci et al., 2002) and rhythmic respiratory bursting activity in brainstem neurons (Hülsmann et al., 2000), and those effects can be restored by glutamine. These various findings suggest that aconitase and the astroglial-dependent glutamine supply to neurons is important in the development of enhanced noxious neuronal activity but not in basal responses, and may therefore be an important factor in exaggerated pain states. The present data are consistent with this view since intrathecal FA markedly attenuated the

hyperexcitability of Vc nociceptive neurons and the associated nocifensive behavior and enhanced GFAP and pERK expression in Vc following trigeminal nerve injury. Furthermore, the expression of hyperactive GFAP-positive cells in Vc is known to last >2 weeks following trigeminal nerve injury (Piao et al., 2006). We also could not observe any significant increase in GFAP immunoproducts in the Vc at 1 d after IAN transection in IANX rats but there was a significant increase in the Vc at 7 d after IAN transection. These findings suggest that astroglial TCA metabolism is involved in the maintenance of hyperexcitability of Vc nociceptive neurons, which is a crucial element in trigeminal nociceptive pathways (Dubner and Bennett, 1983; Bereiter et al., 2000; Sessle, 2000, 2005).

Together with these previous findings, our results suggest that glutamine released from hyperactive astroglia in Vc following trigeminal nerve injury is involved in the increment of nociceptive responses in Vc neurons and the enhanced nocifensive behavior induced by noxious stimulation.

Supplementary Material

Refer to Web version on PubMed Central for supplementary material.

Acknowledgments

References

Allen NJ, Barres BA. Signaling between glia and neurons: focus on synaptic plasticity. Curr Opin Neurobiol 2005;15:542–548. [PubMed: 16144764]

Araque A. Astrocyte-neuron signaling in the brain-implications fordisease. Curr Opin Investig Drugs 2006;7:619–624.

Bacci A, Sancini G, Verderio C, Armano S, Pravettoni E, Fesce R, Franceschetti S, Matteoli M. Block of glutamate-glutamine cycle between astrocytesand neurons inhibits epileptiform activity in hippocampus. J Neurophysiol 2002;88:2302–2310. [PubMed: 12424271]

Bereiter DA, Hirata H, Hu JW. Trigeminal subnucleus caudalis: beyond homologies with the spinal dorsal horn. Pain 2000;88:221–224. [PubMed: 11068108]

Cheng C, Zochodne DW. In vivo proliferation, migration and phenotypic changes of Schwann cells in the presence of myelinated fibers. Neuroscience 2002;115:321–329. [PubMed: 12401344]

Chiang CY, Wang J, Xie YF, Zhang S, Hu JW, Dostrovsky JO, Sessle BJ. Astroglial glutamate–glutamine shuttle is involved in central sensitization of nociceptive neurons in rat medullary dorsal horn. J Neurosci 2007;27:9068–9076. [PubMed: 17715343]

Chiang CY, Li Z, Dostrovsky JO, Hu JW, Sessle BJ. Glutamine uptake contributes to central sensitization in the medullary dorsal horn. Neuro-report 2008;19:1151–1154.

Debus E, Weber K, Osborn M. Monoclonal antibodies specific for glial fibrillary acidic (GFA) protein and for each of the neurofilament triplet polypeptides. Differentiation 1983;25:193–203. [PubMed: 6198232]

Dubner R, Bennett GJ. Spinal and trigeminal mechanisms of nociception. Annu Rev Neurosci 1983;6:381–418. [PubMed: 6132587]

Fitzgerald M. The development of nociceptive circuits. Nat Rev Neurosci 2005;6:507–520. [PubMed: 15995722]

Fonnum F, Johnsen A, Hassel B. Use of fluorocitrate and fluoroacetate in the study of brain metabolism. Glia 1997;21:106–113. [PubMed: 9298853]

Fonseca LL, Monteiro MA, Alves PM, Carrondo MJ, Santos H. Cultures of rat astrocytes challenged with a steady supply of glutamate: new model to study flux distribution in the glutamate-glutamine cycle. Glia 2005;51:286–296. [PubMed: 15834952]

Franke FE, Schachenmayr W, Osborn M, Altmannsberger M. Unexpected immunoreactivities of intermediate filament antibodies in human brain and brain tumors. Am J Pathol 1991;139:67–79. [PubMed: 1713022]

Guo W, Wang H, Watanabe M, Shimizu K, Zou S, LaGraize SC, Wei F, Dubner R, Ren K. Glial-cytokine-neuronal interactions underlying the mechanisms of persistent pain. J Neurosci 2007;27:6006–6018. [PubMed: 17537972]

Haydon PG, Carmignoto G. Astrocyte control of synaptic transmission and neurovascular coupling. Physiol Rev 2006;86:1009–1031. [PubMed: 16816144]

Hertz L, Zielke HR. Astrocytic control of glutamatergic activity: astrocytes as stars of the show. Trends Neurosci 2004;27:735–743. [PubMed: 15541514]

Hülsmann S, Oku Y, Zhang W, Richter DW. Metabolic coupling between glia and neurons is necessary for maintaining respiratory activity in transverse medullary slices of neonatal mouse. Eur J Neurosci 2000;12:856–862. [PubMed: 10762315]

Iwata K, Tashiro A, Tsuboi Y, Imai T, Sumino R, Morimoto T, Dubner R, Ren K. Medullary dorsal horn neuronal activity in rats with persistent temporomandibular joint and perioral inflammation. J Neurophysiol 1999;82:1244–1253. [PubMed: 10482744]

Iwata K, Imai T, Tsuboi Y, Tashiro A, Ogawa A, Morimoto T, Masuda Y, Tachibana Y, Hu J. Alteration of medullary dorsal horn neuronal activity following inferior alveolar nerve transection in rats. J Neuro-physiol 2001;86:2868–2877.

Ji RR. Mitogen-activated protein kinases as potential targets for pain killers. Curr Opin Investig Drugs 2004;5:71–75.

Ji RR, Strichartz G. Cell signaling and the genesis of neuropathic pain. Sci STKE 2004 2004:reE14.

Ji RR, Baba H, Brenner GJ, Woolf CJ. Nociceptive-specific activation of ERK in spinal neurons contributes to pain hypersensitivity. Nat Neurosci 1999;12:1114–1119. [PubMed: 10570489]

Jongen JL, Jaarsma D, Hossaini M, Natarajan D, Haasdijk ED, Holstege JC. Distribution of RET immunoreactivity in the rodent spinal cord and changes after nerve injury. J Comp Neurol 2007;500:1136–1153. [PubMed: 17183535]

Keyser DO, Pellmar TC. Synaptic transmission in the hippocampus: critical role for glial cells. Glia 1994;10:237–243. [PubMed: 7914511]

Martinez-Hernandez A, Bell KP, Norenberg MD. Glutamine synthetase: glial localization in brain. Science 1977;195:1356–1358. [PubMed: 14400]

Milligan ED, Twining C, Chacur M, Biedenkapp J, O'Connor K, Poole S, Tracey K, Martin D, Maier SF, Watkins LR. Spinal glia and proinflammatory cytokines mediate mirror-image neuropathic pain in rats. J Neurosci 2003;23:1026–1040. [PubMed: 12574433]

Newman EA. New roles for astrocytes: regulation of synaptic transmission. Trends Neurosci 2003;26:536–542. [PubMed: 14522146]

Noma N, Tsuboi Y, Kondo M, Matsumoto M, Sessle BJ, Kitagawa J, Saito K, Iwata K. Organization of pERK-immunoreactive cells in trigeminal spinal nucleus caudalis and upper cervical cord following capsaicin injection into oral and craniofacial regions in rats. J Comp Neurol 2008;507:1428–1440. [PubMed: 18196540]

Nomura H, Ogawa A, Tashiro A, Morimoto T, Hu JW, Iwata K. Induction of Fos protein-like immunoreactivity in the trigeminal spinal nucleus caudalis and upper cervical cord following noxious and non-noxious mechanical stimulation of the whisker pad of the rat with an inferior alveolar nerve transection. Pain 2002;95:225–238. [PubMed: 11839422]

Ogawa A, Meng ID. Differential effects of the cannabinoid receptor agonist, WIN 55,212-2, on lamina I and lamina V spinal trigeminal nucleus caudalis neurons. Pain 2009;141:269–275. [PubMed: 19114295]

Perea G, Araque A. Synaptic information processing by astrocytes. J Physiol Paris 2006;99:92–97. [PubMed: 16442272]

Piao ZG, Cho IH, Park CK, Hong JP, Choi SY, Lee SJ, Lee S, Park K, Kim JS, Oh SB. Activation of glia and microglial p38 MAPK in medullary dorsal horn contributes to tactile hypersensitivity following trigeminal sensory nerve injury. Pain 2006;121:219–231. [PubMed: 16495005]

Rosen LB, Ginty DD, Weber MJ, Greenberg ME. Membrane depolarization and calcium influx stimulate MEK and MAP kinase via activation of Ras. Neuron 1994;12:1207–1221. [PubMed: 8011335]

Saito K, Hitomi S, Suzuki I, Masuda Y, Kitagawa J, Tsuboi Y, Kondo M, Sessle BJ, Iwata K. Modulation of trigeminal spinal subnucleus caudalis neuronal activity following regeneration of transected inferior alveolar nerve in rats. J Neurophysiol 2008;99:2251–2263. [PubMed: 18337368]

Schousboe A, Waagepetersen HS. Glial modulation of GABAergic and glutamatergic neurotransmission. Curr Top Med Chem 2006;6:929–934. [PubMed: 16787266]

Schousboe A, Westergaard N, Waagepetersen HS, Larsson OM, Bakken IJ, Sonnewald U. Trafficking between glia and neurons of TCA cycle intermediates and related metabolites. Glia 1997;21:99–105. [PubMed: 9298852]

Sessle BJ. Acute and chronic craniofacial pain: brainstem mechanisms of nociceptive transmission and neuroplasticity, and their clinical correlates. Crit Rev Oral Biol Med 2000;11:57–91. [PubMed: 10682901]

Sessle BJ. Peripheral and central mechanisms of orofacial pain and their clinical correlates. Minerva Anestesiol 2005;71:117–136. [PubMed: 15756153]

Sharma HS. Neuroprotective effects of neurotrophins and melanocortins in spinal cord injury: an experimental study in the rat using pharmacological and morphological approaches. Ann N Y Acad Sci 2005;1053:407–421. [PubMed: 16179548]

Shimizu K, Asano M, Kitagawa J, Ogiso B, Ren K, Oki H, Matsumoto M, Iwata K. Phosphorylation of extracellular signal-regulated kinase in medullary and upper cervical cord neurons following noxious tooth pulp stimulation. Brain Res 2006;1072:99–109. [PubMed: 16442086]

Suzuki I, Harada T, Asano M, Tsuboi Y, Kondo M, Gionhaku N, Kitagawa J, Kusama T, Iwata K. Phosphorylation of ERK in trigeminal spinal nucleus neurons following passive jaw movement in rats with chronic temporomandibular joint inflammation. J Orofac Pain 2007;21:225–231. [PubMed: 17717961]

Swanson RA, Graham SH. Fluorocitrate and fluoroacetate effects on astrocyte metabolism in vitro. Brain Res 1994;664:94–100. [PubMed: 7895052]

Trevino DL, Coulter JD, Willis WD. Location of cells of origin of spinothalamic tract in lumbar enlargement of the monkey. J Neurophysiol 1973;36:750–761. [PubMed: 4197341]

Tsuboi Y, Takeda M, Tanimoto T, Ikeda M, Matsumoto S, Kitagawa J, Teramoto K, Simizu K, Yamazaki Y, Shima A, Ren K, Iwata K. Alteration of thesecond branch of the trigeminal nerve activity following inferior alveolar nerve transection in rats. Pain 2004;111:323–334. [PubMed: 15363876]

Tsuda M, Inoue K, Salter MW. Neuropathic pain and spinal microglia: a big problem from molecules in "small" glia. Trends Neurosci 2005;28:101–107. [PubMed: 15667933]

Watkins LR, Maier SF. Glia: a novel drug discovery target for clinicalpain. Nat Rev Drug Discov 2003;2:973–985. [PubMed: 14654796]

Watkins LR, Martin D, Ulrich P, Tracey KJ, Maier SF. Evidence forthe involvement of spinal cord glia in subcutaneous formalin inducedhyperalgesia in the rat. Pain 1997;71:225–235. [PubMed: 9231865]

Wei F, Guo W, Zou S, Ren K, Dubner R. Supraspinal glial-neuronalinteractions contribute to descending pain facilitation. J Neurosci 2008;28:10482–10495. [PubMed: 18923025]

Xie YF, Zhang S, Chiang CY, Hu JW, Dostrovsky JO, Sessle BJ. Involvement of glia in central sensitization in trigeminal subnucleus caudalis (medullary dorsal horn). Brain Behav Immun 2007;21:634–641. [PubMed: 17055698]

Xu M, Aita M, Chavkin C. Partial infraorbital nerve ligation as a model of trigeminal nerve injury in the mouse: behavioral, neural, and glial reactions. J Pain 2008;9:1036–1048. [PubMed: 18708302]

Zimmermann M. Ethical guidelines for investigations of experimental pain in conscious animals. Pain 1983;16:109–110. [PubMed: 6877845]
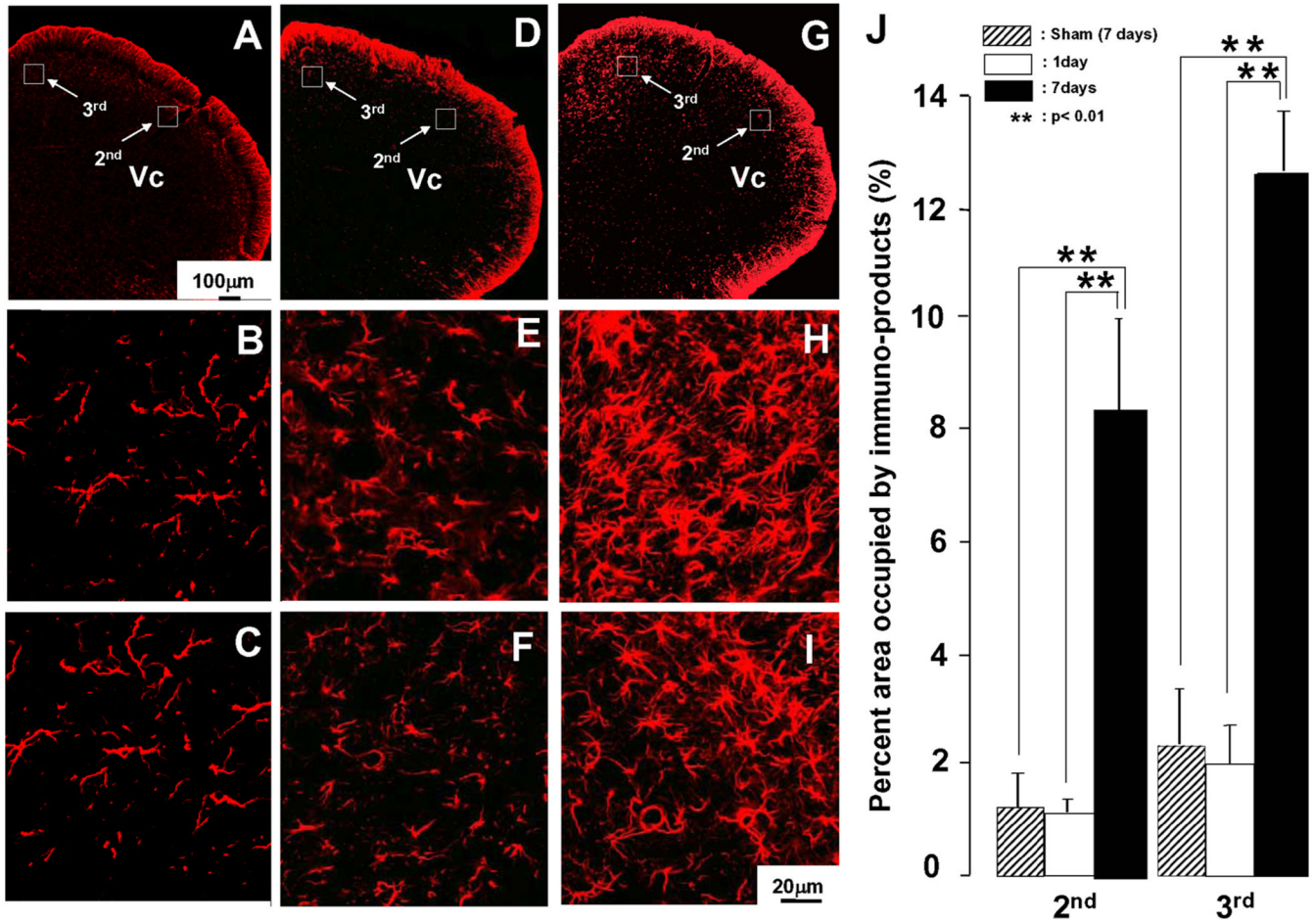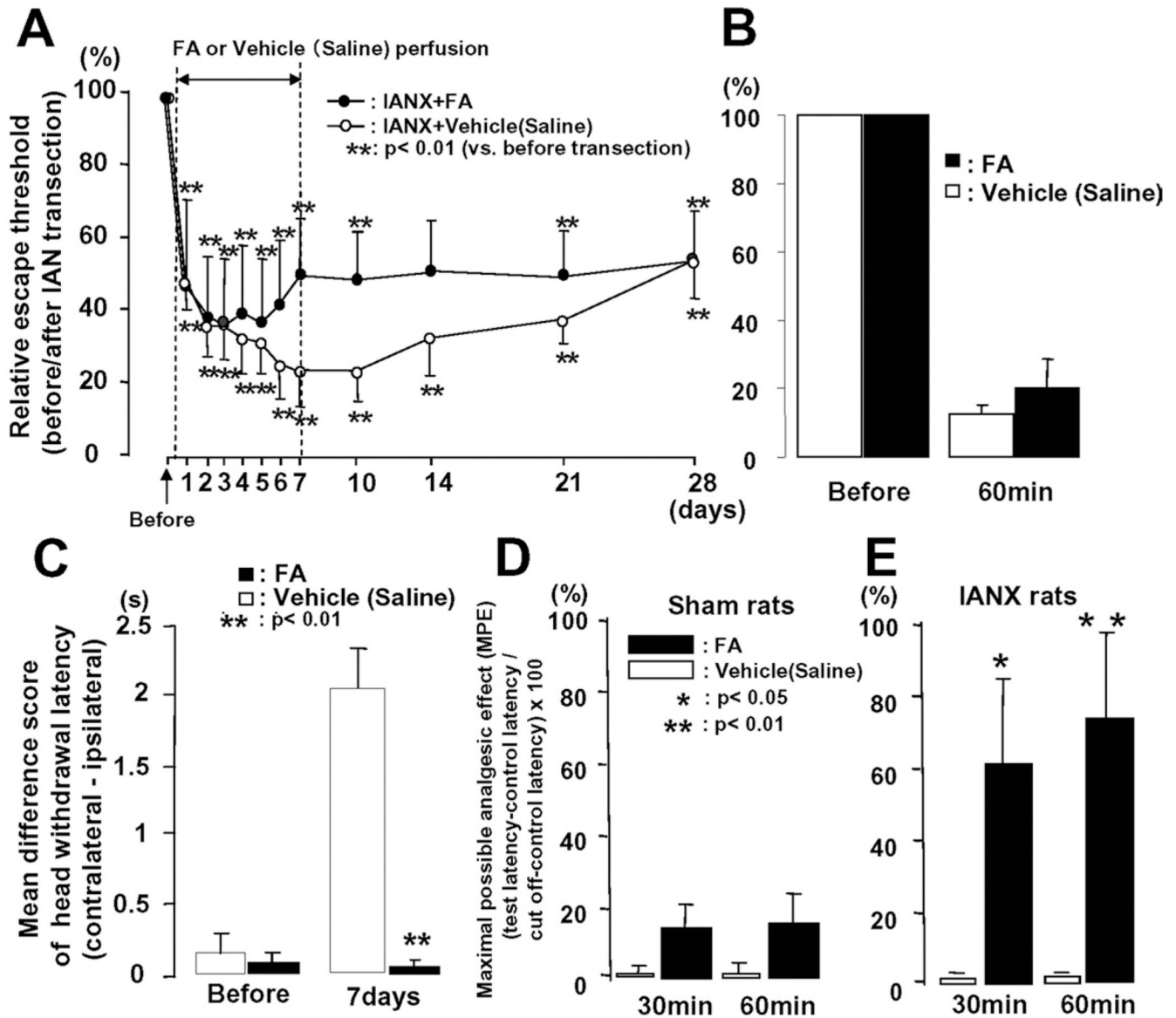
Figure 1.
GFAP-positive cells in Vc of the IANX rats and that from sham-control rats. *A–I*, Low- and high-magnification photomicrographs of Vc in sham-control rats (*A–C*), and in rats 1 (*D–F*) and 7 (*G–I*) d after IAN transection. The percentage area occupied by GFAP-positive cells was analyzed for the dorsal portion of the Vc innervated by third branch of the trigeminal nerve (*B, E, H*) and the middle portion of the Vc innervated by the second branch of the trigeminal nerve (*C, F, I*) (see Noma et al., 2008). Histograms in *J* indicate the relative mean area occupied by GFAP-positive cells in that part of Vc innervated by the second and third branches of the trigeminal nerve, respectively. **$p < 0.01$.
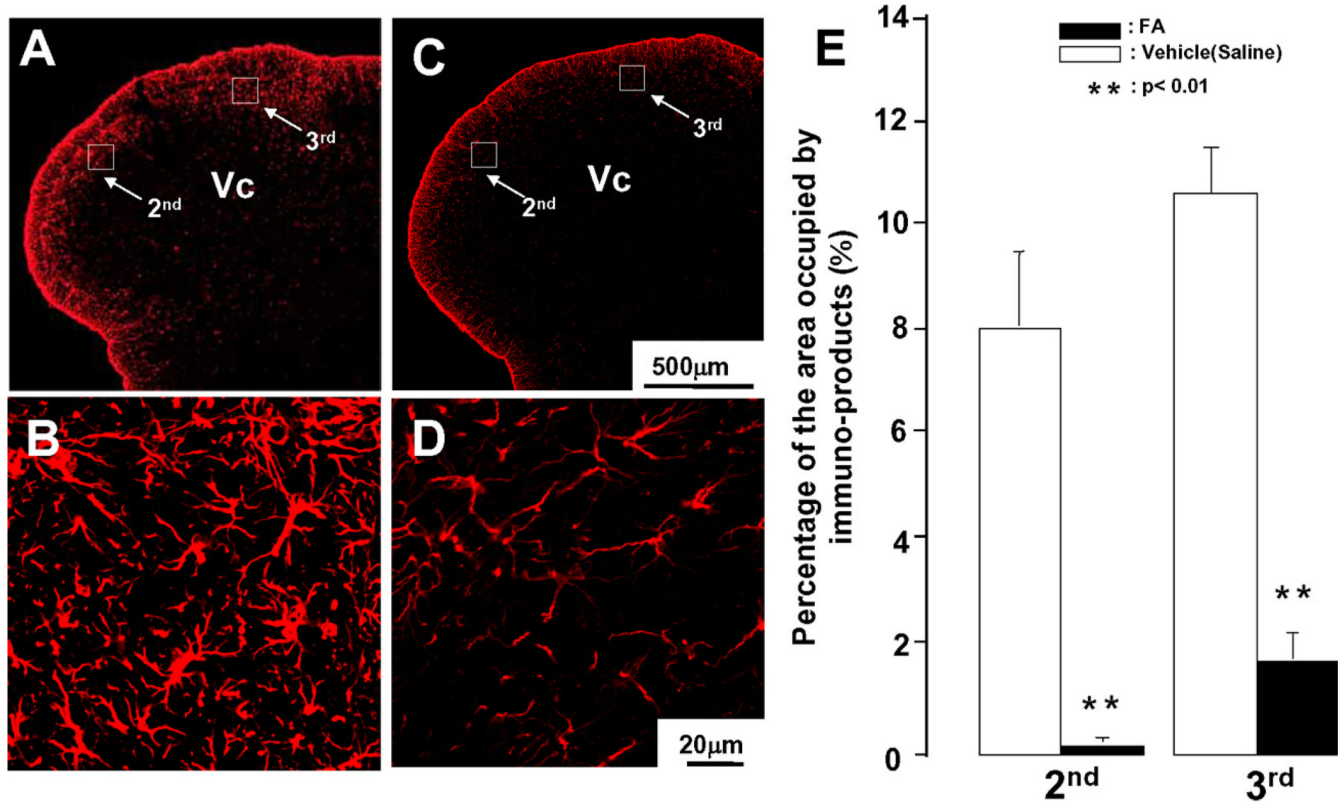
Figure 2.
Effect of intrathecal FA administration on GFAP-positive cells in the Vc of IANX rats. *A, C*,
Low-magnification photomicrographs of GFAP-positive cells in Vc following intrathecal
administration of vehicle (isotonic saline) (*A*) or that after FA administration (*C*) in IANX rats
7 d after IAN transection. *B, D*, High-magnification photomicrograph of the Vc innervated by
the third branch of the trigeminal nerve in the intrathecal vehicle (isotonic saline)-administrated
rat (*B*) and FA-administrated rat (*D*). *E*, Relative area occupied by GFAP-positive cells in Vc
innervated by the second and third branches of the trigeminal nerve in IANX rats. *$p < 0.05$.

Figure 3.
Head withdrawal threshold to low-intensity mechanical stimulation of the maxillary whisker pad skin (*A*: continuous i.t. injection of FA, *B*: i.t. injection of FA at 7 d after IAN transection) and mean differential score of head withdrawal latency to heat stimulation of the whisker pad skin (*C*: continuous i.t. injection of FA) in awake IANX rats and MPE to high-intensity heat stimulation of the maxillary whisker pad skin in lightly anesthetized sham-control (*D*) or IANX (*E*) rats following intrathecal perfusion of FA or vehicle (isotonic saline). The escape threshold to low-intensity mechanical stimulation was significantly reduced after IAN transection compared with that before IAN transection in intrathecal FA- or vehicle (isotonic saline)-perfused rats (*A, B*). Note that no significant changes in escape threshold to low-intensity mechanical stimulation of the maxillary whisker pad were observed in IANX rats following intrathecal FA perfusion for 7 d (solid circles in *A*) and intrathecal single injection of FA at 7 d after IAN transection (*B*). Significant decrease in mean differential score of head withdrawal latency was observed in IANX rats following continuous intrathecal infusion of FA (solid

column in **C**). MPE was significantly increased at 30 and 60 min after intrathecal FA perfusion in IANX rats (solid column in **E**), but was not changed after vehicle (isotonicsaline) administration (open column in **E**) and FA sham-control rats (**D**). MPE value was calculated by the following formula: MPE (%) = (test latency — control latency)/(cutoff — control latency) $\times$ 100. $*p < 0.05$, $**p < 0.01$.
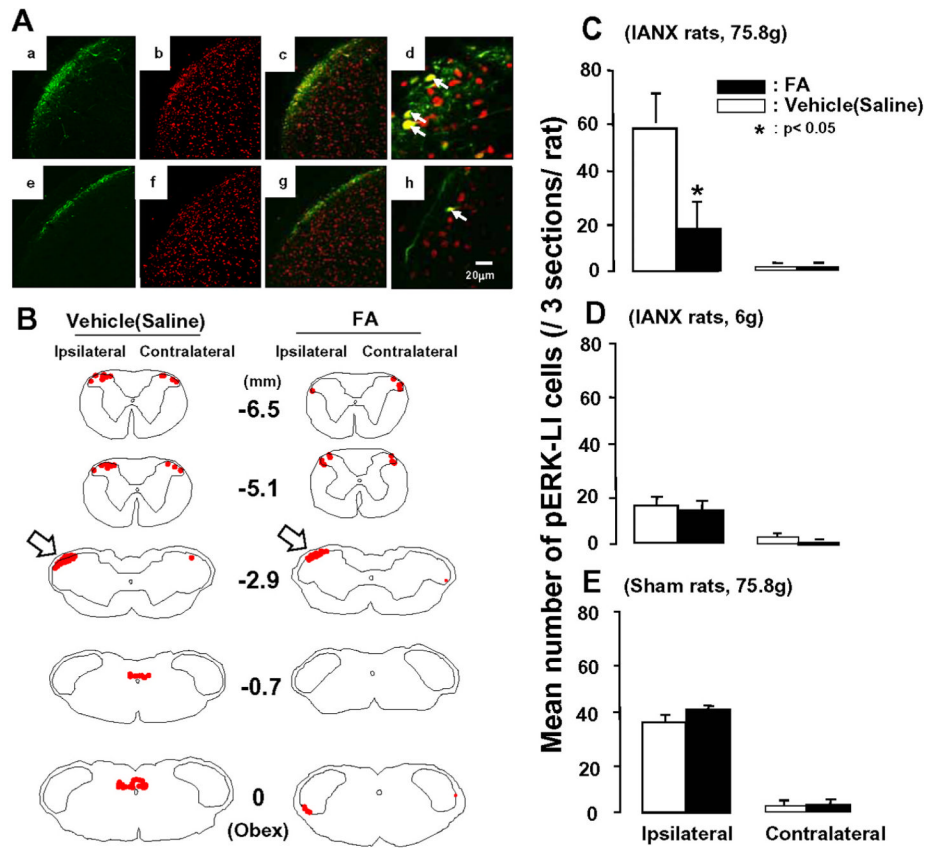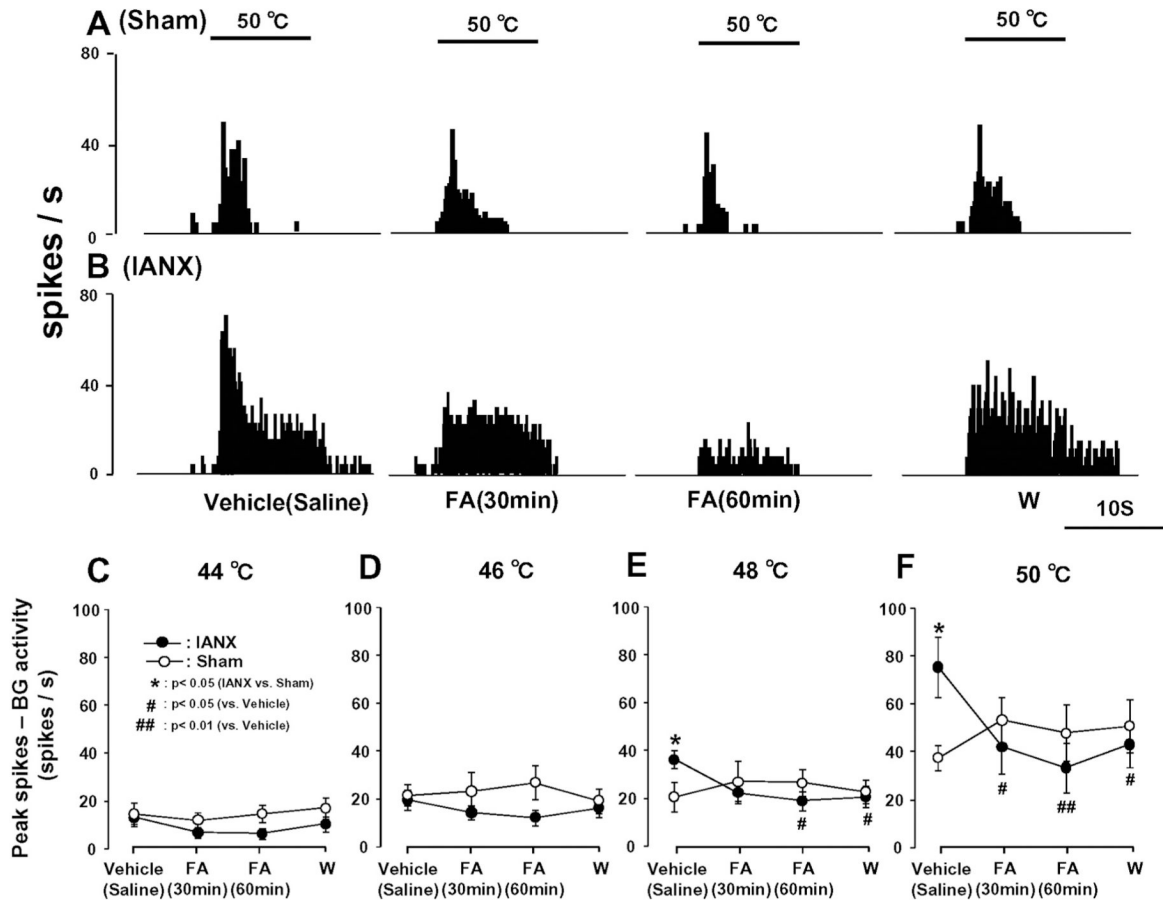
Figure 4.
The effect of intrathecal FA administration on pERK in Vc neurons in IANX and sham-control rats. *A*, Photomicrographs of pERK-LI cells (*a*) and NeuN-positive cells (*b*), merged photomicrograph of *a* and *b* (*c*), and high magnification of *c* (*d*) in IANX rats with intrathecal vehicle (isotonic saline) administration following high-intensity mechanical (75.8 g) stimulation of the maxillary whisker pad and those from IANX rats with intrathecal FA administration (*e–h*). *B*, Camera lucida drawings of pERK-LI cells in Vc and upper cervical spinal cord following high-intensity mechanical stimulation (75.8 g) of the maxillary whisker pad skin in IANX rats with intrathecal vehicle (isotonic saline) or FA administration. Each red dot in the drawings indicates pERK-LI cells in *B*. *C, D*, The effects of intrathecal vehicle (isotonic saline) or FA administration on the number of pERK-LI cells in Vc after high-intensity (75.8 g) (*C*) or low-intensity (6 g) mechanical stimulation of the maxillary whisker pad skin (*D*) in IANX rats. *E*, The effects of intrathecal vehicle (isotonic saline) or FA administration on the number of pERK-LI cells in Vc after high-intensity mechanical (75.8 g) stimulation of the maxillary whisker pad skin in sham-control rats. Arrows in *Ad* and *Ah* indicate pERK-LI cells with NeuN immunoreactivity. Ipsilateral, Ipsilateral side to IAN transection or sham operation; Contralateral, contralateral side to IAN transection or sham operation. The arrows in *B* indicate the Vc region where a large number of pERK-LI cells were expressed. *$p < 0.05$.
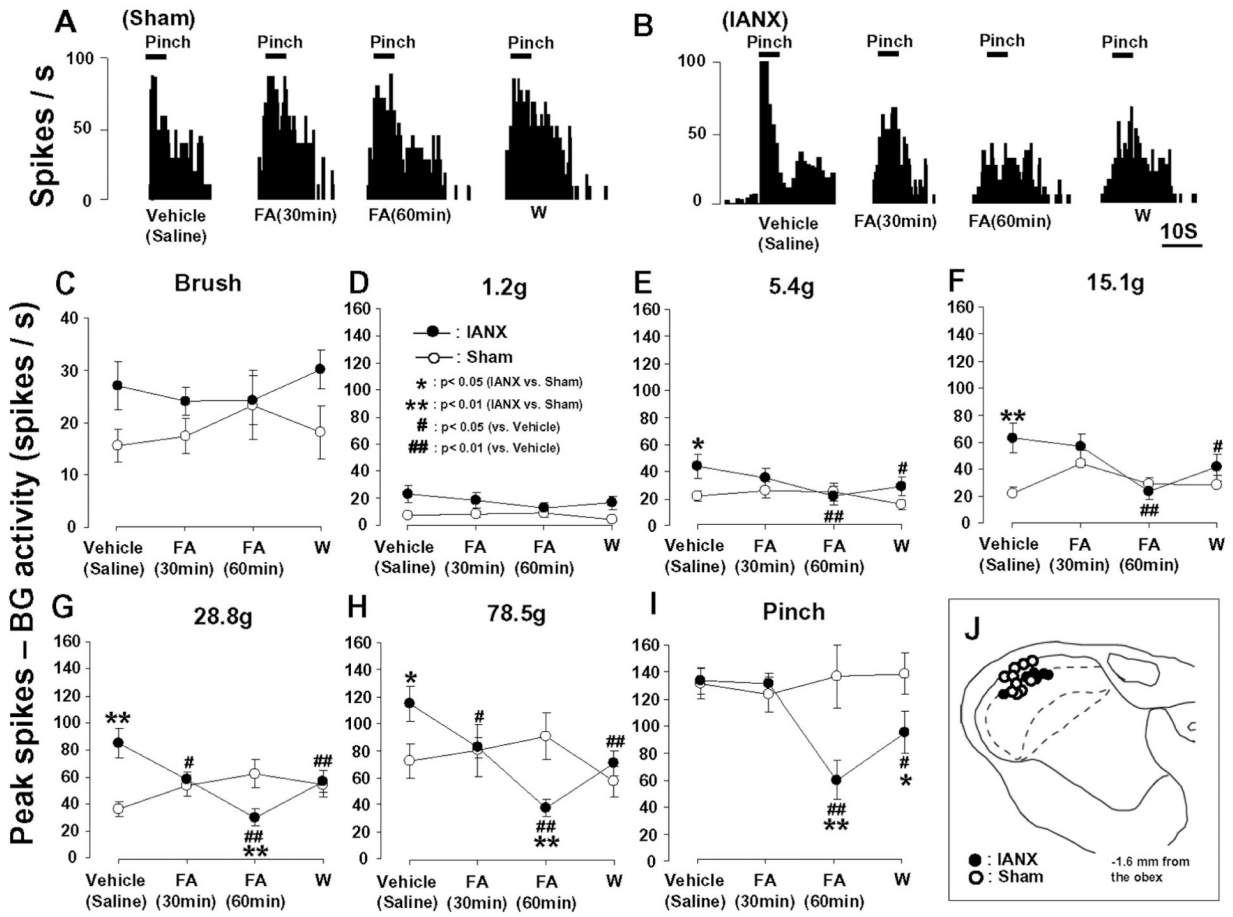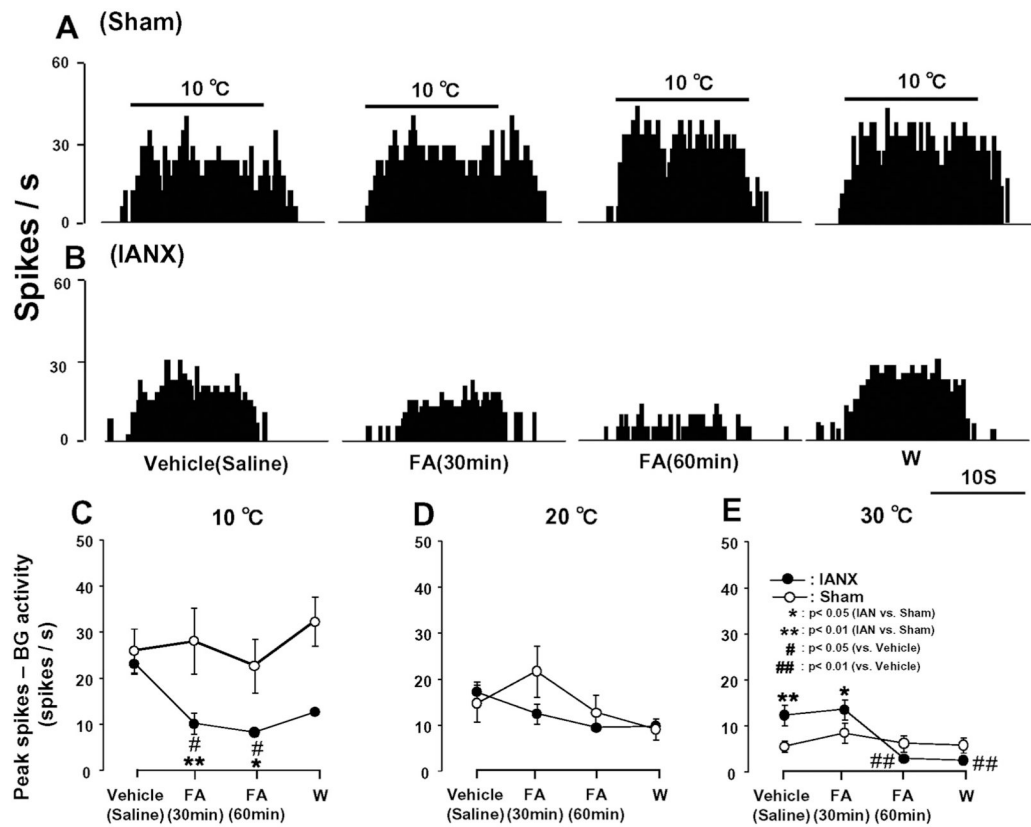
Figure 5.
The effect of intrathecal administration of FA or vehicle (isotonic saline) on pinch-evoked responses of Vc neurons in the IANX or sham-control rats. *A, B*, Typical peristimulus time histograms (PSTHs) of Vc WDR neurons to pinch stimulus of the maxillary whisker pad skin following intrathecal vehicle (isotonic saline) or FA administration in sham-control (*A*) and IANX (*B*) rats; bin width, 500 ms. *C–I*, Response to brushing (*C*), 1.2 g pressure stimulation (*D*), 5.4 g pressure stimulation (*E*), 15.1 g pressure stimulation (*F*), 28.8 g pressure stimulation (*G*), 75.8 g pressure stimulation (*H*), and pinching (*I*) of the RF. *J*, Recording sites. Vehicle (saline), FA (30 min), FA (60 min), and W indicate intrathecal isotonic saline administration, 30 min after intrathecal FA administration, 60 min after intrathecal FA administration, and washout, respectively, in this and Figure 6 and Figure 7. Bars in *A* indicate the duration of pinching of the maxillary whisker pad skin. *$p < 0.05$, **$p < 0.01$ (IANX rats vs sham-control rats); #$p < 0.05$, ##$p < 0.01$ (vs vehicle-administrated rats). BG, Background.
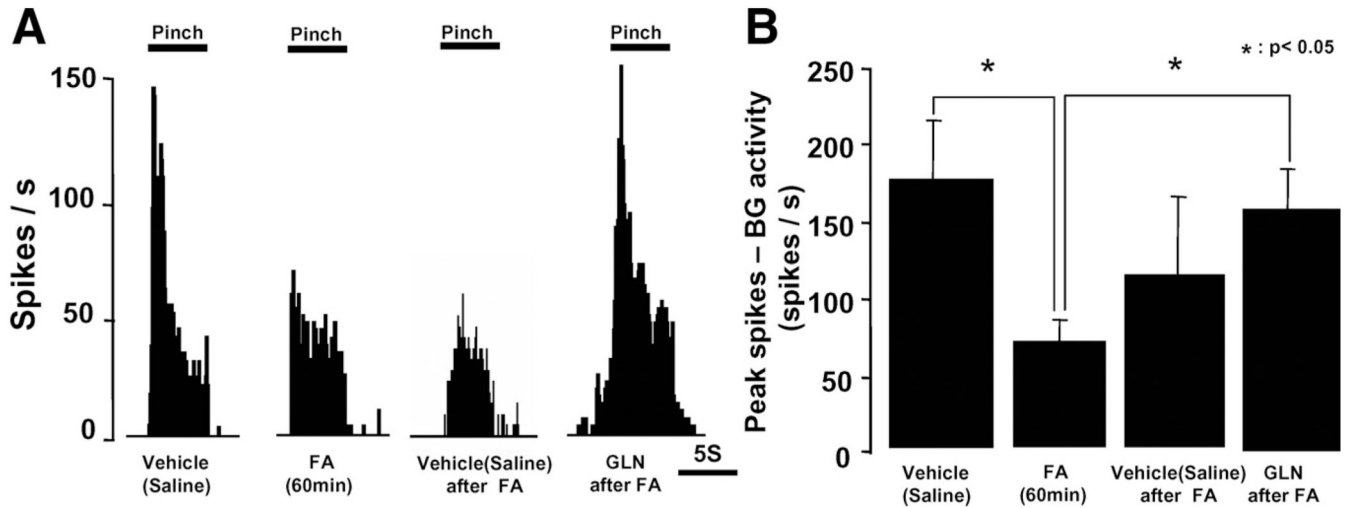
Figure 6.
The effect of intrathecal FA administration on high-intensity heat-evoked responses in IANX rats. *A, B*, PSTHs of Vc WDR neurons following 50°C stimulation of the maxillary whisker pad skin in sham-control rats (*A*) and IANX rats (*B*) at 30 and 60 min after start of FA perfusion and following washout (W). *C–F*, Response to 44°C (*C*), 46°C (*D*), 48°C (*E*), and 50°C (*F*) stimulation of the RF. Bars in *A* indicates the duration of 50°C stimulus of the maxillary whisker pad. Sham, Sham operation. *$p < 0.05$ (IANX rats vs sham-control rats); #$p < 0.05$, ##$p < 0.01$ (vs vehicle-administrated rats).

Figure 7.
The effect of intrathecal FA administration on high-intensity cold-evoked responses in IANX rats. *A, B*, PSTHs of Vc WDR neurons following 10°C stimulation of the maxillary whisker pad skin in sham-control rats (*A*) and IANX rats (*B*). *C–E*, Response to 10°C (*C*), 20°C (*D*), and 30°C (*E*) stimulation of the RF. Bars in *A* indicate the duration of 10°C stimulation of the maxillary whisker pad skin. *$p < 0.05$, **$p < 0.01$ (IANX rats vs sham-control rats); #$p < 0.05$, ##$p < 0.01$ (vs vehicle-administrated rats). See Figure 6 legend for further details.

Figure 8.
The effect of topical glutamine infusion on pinch-evoked responses in Vc WDR neurons. *A*, A typical PSTH of pinch-evoked responses of a Vc WDR neuron following a series of intrathecal vehicle (isotonic saline), FA, vehicle (isotonicsaline) after FA, and glutamine administrations. *B*, Mean peak firings of pinch-evoked responses of Vc WDR neurons following intrathecal vehicle (isotonic saline), FA, vehicle (isotonic saline) after FA, or glutamine administration. FA (60 min), 60 min after intrathecal FA administration; GLN, glutamine. Bars in *A* indicate the duration of the stimulus. *$p < 0.05$.